

Enriched environment boosts the post-stroke recovery of neurological function by promoting autophagy

<https://doi.org/10.4103/1673-5374.297084>

Yi-Hao Deng[#], Ling-Ling Dong[#], Yong-Jie Zhang, Xiao-Ming Zhao, Hong-Yun He^{*}

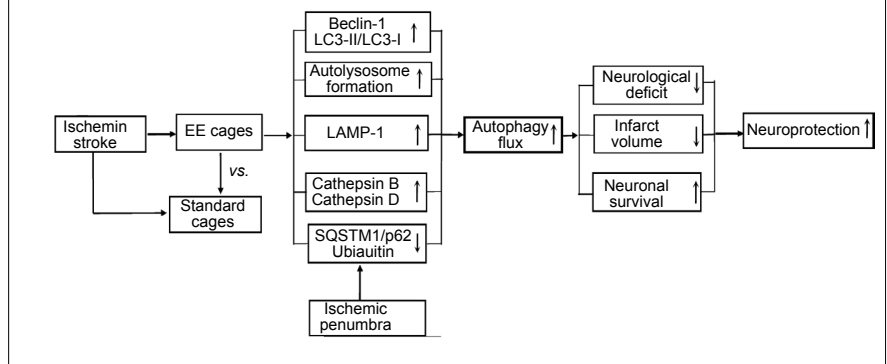
Date of submission: March 25, 2020

Date of decision: April 20, 2020

Date of acceptance: June 6, 2020

Date of web publication: November 16, 2020

Graphical Abstract *Enriched environment (EE) elicits a neuroprotection against ischemic stroke by enhancement of autophagic flux*



Abstract

Autophagy is crucial for maintaining cellular homeostasis, and can be activated after ischemic stroke. It also participates in nerve injury and repair. The purpose of this study was to investigate whether an enriched environment has neuroprotective effects through affecting autophagy. A Sprague-Dawley rat model of transient ischemic stroke was prepared by occlusion of the middle cerebral artery followed by reperfusion. One week after surgery, these rats were raised in either a standard environment or an enriched environment for 4 successive weeks. The enriched environment increased Beclin-1 expression and the LC3-II/LC3-I ratio in the autophagy/lysosomal pathway in the penumbra of middle cerebral artery-occluded rats. Enriched environment-induced elevations in autophagy activity were mainly observed in neurons. Enriched environment treatment also promoted the fusion of autophagosomes with lysosomes, enhanced the lysosomal activities of lysosomal-associated membrane protein 1, cathepsin B, and cathepsin D, and reduced the expression of ubiquitin and p62. After 4 weeks of enriched environment treatment, neurological deficits and neuronal death caused by middle cerebral artery occlusion/reperfusion were significantly alleviated, and infarct volume was significantly reduced. These findings suggest that neuronal autophagy is likely the neuroprotective mechanism by which an enriched environment promotes recovery from ischemic stroke. This study was approved by the Animal Ethics Committee of the Kunming University of Science and Technology, China (approval No. 5301002013855) on March 1, 2019.

Key Words: autophagy; brain; central nervous system; factor; injury; pathways; protection; regeneration; repair; stroke

Chinese Library Classification No. R459.9; R741; Q142

Introduction

Cerebral stroke, a serious cerebrovascular condition, is the second leading cause of death and permanent disability worldwide (Benjamin et al., 2019; Wang et al., 2019; Gao et al., 2020). Approximately 80% of clinical stroke is caused by cerebrovascular occlusion resulting in cerebral ischemia (Wang et al., 2017). Tissue-type plasminogen activator is the only U.S. Food and Drug Administration-approved drug for the treatment of ischemic stroke (Montalván Ayala et al., 2018); however, only about 5% of patients can receive this treatment because of its narrow therapeutic time window (less than 4.5 hours) and adverse side effects (e.g., severe hemorrhage) (Leng and Xiong, 2019). To mitigate neurological deficits and

improve quality of life for stroke survivors, the enhancement of post-stroke rehabilitation is a viable option (Krueger et al., 2015). Investigations have shown that post-stroke recovery can be improved and accelerated by either exercise training or multisensory stimulation (Hakon et al., 2018). Enriched environment (EE) is a rehabilitation strategy that can be used in rodents (Mering and Jolkkonen, 2015). Accumulating evidence has shown that EE exposure after cerebral stroke can improve neurological outcomes by reducing neuronal apoptosis (Chen et al., 2017b), facilitating motor function recovery (Jeffers and Corbett, 2018), promoting neurogenesis (Zhang et al., 2018), inducing astrocytic proliferation (Chen et al., 2017a), and altering gene expression (Gonçalves et al., 2018). One study even showed that prior exposure to EE

Department of Basic Medicine, Medical School, Kunming University of Science and Technology, Kunming, Yunnan Province, China

*Correspondence to: Hong-Yun He, MD, 18487158200@163.com.

<https://orcid.org/0000-0002-5736-146X> (Hong-Yun He)

[#]Both authors contributed equally to this work.

Funding: This work was supported by the National Natural Science Foundation of China, Nos. 81660383 (to YHD), 81860411 (to HYH), 81960418 (to YHD); Yunnan Ten Thousand Talents Plan Young & Elite Talents Project of China, No. YNWR-QNBJ-2018-034 (to YHD); Applied Basic Research Foundation of Yunnan Province of China, Nos. 2017FB113 (to YHD), 2019FB098 (to HYH); and Science Research Fund of Yunnan Provincial Department of Education of China, No. 2018JS016 (to HYH).

How to cite this article: Deng YH, Dong LL, Zhang YJ, Zhao XM, He HY (2021) Enriched environment boosts the post-stroke recovery of neurological function by promoting autophagy. *Neural Regen Res* 16(5):813-819.

Research Article

resulted in greater ischemic tolerance in an animal stroke model (Yu et al., 2013). However, the mechanisms by which EE treatment affects the pathological development of cerebral stroke have not been fully elucidated.

Autophagy is a catabolic mechanism by which damaged organelles, long-lived proteins, and cytoplasmic contents are delivered to lysosomes for degradation (Wang et al., 2018). Autophagy is critical for the maintenance of cellular homeostasis in the brain under physiological conditions. It also protects cells from injury under pathological conditions by eliminating pathogens, toxins, and aberrant cytoplasmic components (Galluzzi et al., 2016). One study has demonstrated that autophagy enhancement can alleviate cerebral ischemia-induced neurological injury (Sun et al., 2018); in contrast, numerous studies have reported that autophagy activation aggravates ischemic lesions and even leads to autophagic cell death (Button et al., 2015). Thus, autophagy has been suggested to be a double-edged sword in the pathological processes of cerebral stroke (Wei et al., 2012). The process of autophagy involves several consecutive processes: autophagosome formation, fusion of the autophagosome with lysosomes, and autophagosomal degradation within the lysosomes (Zhi et al., 2018). The integrity of these autophagic processes, also known as autophagic flux, is very important for restoring cellular homeostasis (Lahiri et al., 2019). Thus, autophagic degradation in the lysosomes is a critical step for the final elimination of autophagic cargo, and lysosomal function plays a key role in autophagy (Gatica et al., 2018). Therefore, both autophagosome biogenesis and lysosomal function need to be simultaneously assessed when evaluating the roles of autophagy. The present study aimed to verify whether EE treatment could boost recovery from ischemic stroke, and then investigated whether this rehabilitative effect was induced by modulating the autophagic/lysosomal pathway.

Materials and Methods

Experimental animals

All animal experiments in this study were approved by the Animal Experiment Committee of Kunming University of Science and Technology (approval No. 5301002013855) on March 1, 2019. Specific-pathogen-free male Sprague Dawley rats (aged 9–10 weeks old, weighing 250–280 g) were purchased from Hunan Slac Laboratory Animal Corporation (license No. SCXK (Xiang) 2016-0002). The animals were fed in accordance with animal welfare practices. The rats were housed in a 12-hour light/dark cycle (light period from 8:00 to 20:00) in a controlled environment (60 ± 5% relative humidity, 21 ± 1°C), and were given free access to food and fresh water. Every effort was made to reduce the number of rats used and alleviate any pain.

A total of 109 rats were used; of these, 19 rats died during or after the surgical operation (the mortality rate was 17.43%). The 90 remaining rats were randomly divided into three equal groups: middle cerebral artery occlusion (MCAO) + EE, MCAO, and sham (sham + EE) groups. In each group, 6 rats were used for detecting autophagic/lysosomal pathway proteins by western blot, 6 animals were used for immunofluorescence staining following the measurement of neurological scores, and the remaining 6 rats were used to measure infarct volume via triphenyltetrazolium chloride (TTC) staining.

Establishment of rat cerebral ischemia/reperfusion injury model

The rat model of cerebral ischemia/reperfusion injury was prepared according to our previous study (Pengyue et al., 2017). Briefly, the left common carotid artery, external carotid artery, and internal carotid artery were isolated from adjacent tissue in rats under deep anesthesia with 10% chloral hydrate (400 mg/kg; intraperitoneal injection; Sigma, St. Louis, MO,

USA). A 4-0 nylon monofilament with a poly-L-lysine-coated head (Beijing Xinong Biotechnology Co., Ltd., Beijing, China) with a tip diameter of approximately 0.36 mm (similar to the diameter of the middle cerebral artery of rats weighing 250–280 g) (He et al., 2019) was introduced from the left common carotid artery into the internal carotid artery through a small incision on the external carotid artery. The nylon monofilament was then advanced 20 ± 1 mm into the left MCAO, and a timer was started immediately. At 90 minutes after MCAO, the nylon monofilament was gently removed for reperfusion to occur. The sham surgery rats received the same operation, but the nylon monofilament was not inserted.

EE procedure

Before MCAO, the rats were kept in the EE cages for 1 week, and received daily training to learn to obtain food on the second floor. One week after reperfusion, the rats were exposed to the EE. This delayed time point (1 week post-stroke) was chosen based on indications from reported human trials and animal experiments (Farrell et al., 2001; Langhorne et al., 2017), which have demonstrated that neural injury is aggravated if a rehabilitative stimulation is initiated within the first few days after cerebral stroke. The EE treatment lasted for 4 weeks. The EE cages were 85 cm × 50 cm × 50 cm, and each cage contained 10–12 rats to enhance social stimulation. The cages were equipped with different toys, ladders, plastic tunnels, colored blocks, tubes, platforms at different levels, and chains to reinforce cognitive and sensorimotor stimulations (**Figure 1**). The contents of the EE cages were changed every 2 days to increase their novelty and complexity. The standard cages were 40 cm × 30 cm × 20 cm, and each cage contained four rats.

Western blot assay for proteins in the autophagic/lysosomal pathway

After 4 weeks of EE treatment, the rats were sacrificed under deep anesthesia. Brain tissue from the penumbral area was rapidly isolated on ice and incubated with radioimmunoprecipitation assay buffer (Beyotime Biotechnology, Shanghai, China) for 40 minutes. The supernatants were obtained after centrifuging for 15 minutes at 12,000 × *g* at 4°C. Additionally, the insoluble sequestosome 1 (SQSTM1)/p62 in the lysates was obtained using an inclusion body solubilization buffer kit (Shanghai Sangon Biotechnology Co., Ltd., Shanghai, China) according to the manufacturer's instructions. The proteins were isolated using sodium dodecyl sulphate-polyacrylamide gel electrophoresis and transferred to polyvinylidene fluoride membranes (Millipore, Billerica, MA, USA). To block nonspecific reactions, the polyvinylidene fluoride membranes were treated with 10% nonfat milk for 2 hours, and then washed with phosphate-buffered saline (PBS) containing 0.1% Tween-20. Rabbit antibodies against rat Beclin-1 (1:1000; Cell Signaling Technology, Danvers, MA, USA), light chain 3 (LC3; 1:1000; Cell Signaling Technology), SQSTM1/p62 (1:1000; Cell Signaling Technology), ubiquitin (1:1000; Cell Signaling Technology), cathepsin B (a main lysosomal protease (Kaminsky and Zhivotovsky, 2012); 1:1000; Santa Cruz Biotechnology, Dallas, TX, USA), cathepsin D (a main lysosomal protease (Kaminsky and Zhivotovsky, 2012); 1:1000; Santa Cruz Biotechnology), lysosomal-associated membrane protein 1 (LAMP-1, a marker of lysosomal homeostasis (Wu et al., 2019); 1:700; ABClonal Technology, Wuhan, China) and β-actin (1:1000; Cell Signaling Technology) were added for incubation at 4°C overnight. After washing with PBS containing 0.1% Tween-20, the membranes were incubated with horseradish peroxidase-conjugated secondary antibodies against rabbit IgG (1:5000; Cell Signaling Technology) at room temperature for 1 hour. After a 2-hour wash, the reaction bands were stained using electrochemiluminescence. The optical density of the bands was quantified by Image Lab 4.1 (Bio-Rad, Hercules, CA, USA).

Band density values were normalized to β -actin.

Immunofluorescence

After 4 weeks of EE treatment, the rats were anesthetized with 10% chloral hydrate and fixed by transcranial perfusion with physiological saline followed by 4% paraformaldehyde (Invitrogen, Shanghai, China). Brains were quickly removed, dehydrated in 30% sucrose solution for 24 hours, and then cut into 20 μ m sections with a freezing microtome (SLEE, Mainz, Germany). After three 5-minute washes with 0.01 M PBS, sections were permeabilized for 15 minutes with 0.2% Triton X-100 in PBS and blocked for 1 hour with 10% bovine serum albumin (Sigma) in PBS. Sections were then incubated at room temperature for 1 hour with rabbit antibody against rat NeuN (a neuron marker (Mo et al., 2019); 1:400; Abcam, Cambridge, UK), glial fibrillary acidic protein (GFAP; an astrocyte marker (Han et al., 2020); 1:400; Cell Signaling Technology), ionized calcium-binding adaptor molecule 1 (Iba-1; a microglia marker (Skowrońska et al., 2019); 1:400; Abcam), p62 (1:300; Cell Signaling Technology) and LAMP-1 (1:200; Abclonal Technology), and mouse antibodies against rat LC3 (an indicator of autophagy formation (He et al., 2019); 1:300; Cell Signaling Technology) and cathepsin B (1:300; Santa Cruz Biotechnology). After washing, these antibodies were then correspondingly labeled with Alexa Fluor-488-conjugated anti-mouse IgG (1:800; Invitrogen) and Alexa Fluor-594-conjugated anti-rabbit IgG (1:800; Invitrogen) for 2 hours at room temperature in the dark. After a wash step, sections were labeled with 4',6-diamidino-2-phenylindole (1:1000; Invitrogen) for 5 minutes in the dark. After washing, reactions were detected using a fluorescent microscope (Nikon Instruments Co., Ltd., Tokyo, Japan). The percentage of positive cells were calculated. At a high magnification (400 \times), the total number of cells and the number of positive cells were counted in 10 randomly selected penumbral areas in each brain section. Five sections were counted from each rat.

Detection of neuronal survival

Brain tissue was obtained and sectioned as described in the immunofluorescence methods. The sections were first incubated with mouse anti-rat NeuN antibody (1:400; Abcam) for 1 hour at room temperature, and then with Alexa Fluor-488-conjugated anti-mouse IgG (1:800; Invitrogen) for 2 hours at room temperature. Next, the sections were counterstained with 4',6-diamidino-2-phenylindole. The results are expressed as the percentages of NeuN-positive cells. At a high magnification (400 \times), the total number of cells and the number of NeuN-positive neurons were counted in 10 randomly selected penumbral areas of each section. Five sections were counted from each sample.

Modified neurological severity score

Neurological deficits were assessed using the modified neurological severity score (mNSS) (Chen et al., 2017a) at 4 weeks after EE treatment. The mNSS test contained four parts: motor function, including abnormal movement and muscle status; sensory function, including proprioceptive, tactile, and visual deficits; reflex evaluation; and balance ability. The highest possible score was 18, indicating the most severe neurological deficit, while a score of 0 indicated no neurological deficit. That is, a higher score implies a more serious neurological injury.

Measurement of cerebral infarction volume

After mNSS testing, the rats were sacrificed under deep anesthesia. The brains were rapidly removed on ice and immediately frozen for 20 minutes at -20°C before being sliced into 2 mm slices. These brain slices were immediately stained with TTC (2% in PBS; Beijing Solarbio Science & Biotechnology Co., Ltd., Beijing, China) for 45 minutes at

room temperature, and were then fixed for 12 hours in 4% paraformaldehyde buffer (Shanghai Sangon Biotechnology Co., Ltd.). Adobe Photoshop 7.0 (Adobe Systems, Dublin, Ireland) was used to calculate infarct volume, and the results were evaluated as follows: infarction rate (%) = $A^{\circ}/A' \times 100$, in which A' represents the volume of the ipsilateral hemisphere and A° represents the infarct volume.

Statistical analysis

Data are expressed as the mean \pm standard error of the mean (SEM). Statistical differences were evaluated using one-way analysis of variance followed by Dunnett's test, and were analyzed with SPSS 11.0 software (SPSS, Chicago, IL, USA). $P < 0.05$ was taken as statistical significance.

Results

EE treatment increases autophagic activity in the penumbra in an ischemic stroke rat model

After EE treatment, autophagic activity in the penumbra was detected by western blot using antibodies against Beclin-1 (Figure 2A and B) and LC3 (Figure 2A and C). The ratio of LC3-II/LC3-I in the MCAO group was increased compared with the sham group ($P < 0.05$), but the levels of Beclin-1 expression were similar between these two groups ($P > 0.05$). Furthermore, both Beclin-1 expression and the ratio of LC3-II/LC3-I were significantly elevated in the MCAO + EE group compared with the MCAO group ($P < 0.05$).

EE-induced elevated autophagic activity is mainly observed in neurons

To investigate the cellular localization of the EE-induced increase in autophagic activity, double immunofluorescence was performed using antibodies against NeuN, GFAP, Iba-1, and LC3-II (Figure 3A–C). The percentage of LC3-II-/NeuN-positive cells was significantly higher in the MCAO + EE group than in the MCAO group ($P < 0.01$), but was not significantly different between the MCAO and sham groups ($P > 0.05$; Figure 3D). In contrast, the percentages of LC3-II-/GFAP- and LC3-II-/Iba-1-positive cells in the MCAO + EE group were similar to those in the MCAO group ($P > 0.05$; Figure 3E and F). Together, these results suggest that the EE-induced increase in autophagic activity occurred mainly in neurons.

EE treatment facilitates autophagic flux after ischemic stroke

To explore the effects of EE on autophagic flux, western blot was used to detect proteins in the autophagy/lysosomal pathway. The expression levels of autophagy/lysosome pathway proteins were similar between the MCAO and sham groups ($P > 0.05$). However, both Beclin-1 expression and the ratio of LC3-II/LC3-I were significantly higher in the MCAO + EE group than in the MCAO group ($P < 0.05$). Furthermore, the lysosomal activities of LAMP-1, cathepsin B, and cathepsin D were markedly increased by EE treatment ($P < 0.05$, vs. MCAO group; Figure 4A and E–G). In contrast, the autophagic cargoes of ubiquitin (Figure 4A and D) and p62 (Figure 4A–C) were reduced in the MCAO + EE group compared with the MCAO group ($P < 0.05$).

EE treatment boosts autolysosomal function after stroke

The cells in the penumbra were co-labeled with LC3-II/LAMP-1 and p62/cathepsin B by double immunofluorescence (Figure 5A and B). The percentages of both LC3-II-/LAMP-1- and p62-/cathepsin B-positive cells were significantly increased in the MCAO + EE group compared with the MCAO group. This result indicates that autolysosomal function may be enhanced by EE treatment. The percentage of LC3-II-/LAMP-1-positive cells was also higher in the MCAO group than in the sham group ($P < 0.01$), while the ratio of p62-/cathepsin B-positive cells was only slightly higher in the MCAO group than in the sham group ($P < 0.01$; Figure 5C and D).

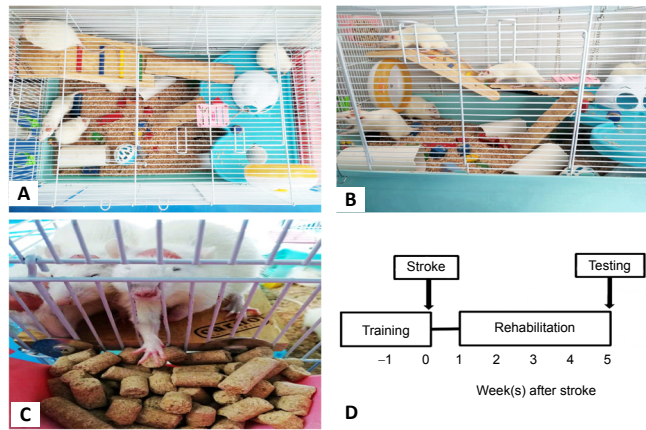


Figure 1 | Rehabilitation apparatus of the enriched environment (EE) and experimental timeline.

(A, B) Superior (A) and lateral (B) view of an EE cage. (C) To take food, rats had to climb up to the highest platform of the EE and grab the food with two forelimbs; thus, the ischemic stroke-impaired limbs were repeatedly stimulated during EE treatment. (D) Timeline of the experimental procedure.

Ischemia-induced neurological deficits are alleviated by EE treatment

The mNSS test was performed to evaluate the effects of EE treatment on neurological deficits caused by MCAO/reperfusion. Neurological deficits were significantly alleviated by 4 weeks of EE treatment (in the MCAO + EE group) compared with the MCAO group ($P < 0.001$). None of the rats in the sham group had neurological deficits (Figure 6).

MCAO-induced infarction is attenuated by EE treatment

After 4 weeks of EE treatment, the TTC results showed that infarct volume in the MCAO + EE group was markedly reduced compared with the MCAO group ($P < 0.001$). None of the rats in the sham group had cerebral infarction (Figure 7).

Neuronal survival is improved by EE treatment

Neuronal survival in the penumbra was detected using immunofluorescence with antibodies against NeuN. The percentage of NeuN-positive cells in the MCAO group was significantly reduced compared with the sham group ($P < 0.01$). However, neuronal survival was markedly improved by 4 weeks of EE treatment ($P < 0.01$, vs. MCAO group; Figure 8). This result indicates that EE treatment can attenuate neuronal death caused by cerebral ischemia.

Discussion

Both clinical trials and animal experiments have demonstrated that exercise training can ameliorate neurological deficits and boost post-stroke recovery by enhancing motor stimulation (Connell et al., 2018; Wright et al., 2018). However, it is not a satisfactory rehabilitation strategy for stroke survivors, because social, cognitive, and sensory stimulations are also necessary to elicit better neurological outcomes. EE not only provides social stimulation by housing many animals in a large space, but it also confers sensorimotor stimulations, with tubes to go through, ladders and platforms to climb, and roller toys to rotate. Moreover, EE cages also augment cognitive stimulation by providing different toys and colored blocks to explore (Gonçalves et al., 2018). Thus, EE treatment is considered an effective rehabilitation treatment for cerebral stroke, and has been shown to elicit neuroprotection against ischemic brain injury (Malá and Rasmussen, 2017; Gonçalves et al., 2018). However, few investigations have elucidated how EE affects the pathological processes of cerebral stroke to elicit neuroprotection (Zhang et al., 2017). Autophagy was initially considered a cellular catabolic mechanism to eliminate injured organelles and residual cellular components

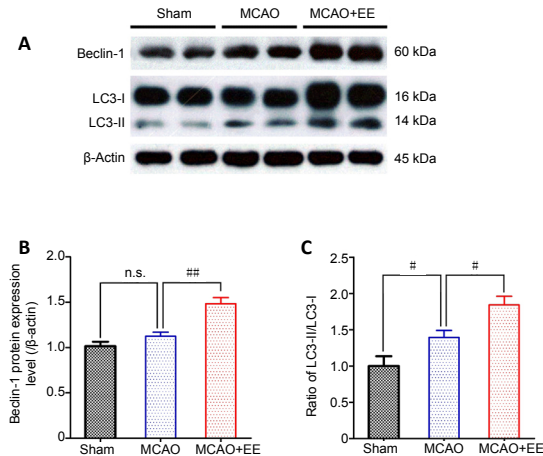


Figure 2 | Effects of EE treatment on autophagic activity in the penumbra of ischemic stroke rats as detected by western blot assay.

MCAO + EE group: MCAO animals were housed in EE cages; MCAO group: MCAO rats were housed in standard cages; sham group: sham surgery rats were housed in EE cages. (A) Protein bands. (B, C) Quantitative results of Beclin-1 protein expression and ratio of LC3-II/LC3-I. Data are expressed as the mean ± SEM of the ratio to the sham group ($n = 6$). # $P < 0.05$, ## $P < 0.01$ (one-way analysis of variance followed by Dunnett’s test). EE: Enriched environment; LC3: light chain 3; MCAO: middle cerebral artery occlusion; n.s.: no significance.

for the maintenance of normal cellular functions and homeostasis. More recently, however, multiple studies have shown that autophagy is strongly activated and has a vital role in the promotion of cell survival after cerebral stroke (Wang et al., 2018). Given that both EE treatment and activated autophagy are reportedly involved in neuroprotection after cerebral stroke, we hypothesized that there was likely a close correlation between them in the facilitation of post-stroke recovery. In the present study, we therefore investigated whether EE-elicited neuroprotection after ischemic stroke had an autophagic mechanism.

Our study demonstrated that EE treatment markedly attenuated neurological deficits, infarct volume, and neuronal death after MCAO, suggesting that EE treatment reliably elicits neuroprotection against cerebral ischemia/reperfusion injury. These results were consistent with the outcomes of previously published studies (Chen et al., 2017a; Qian et al., 2018). To investigate whether EE-induced neuroprotection was elicited by targeting autophagic flux, we detected key proteins in the autophagic flux pathway. Western blot results demonstrated that EE treatment significantly promoted the expression of Beclin-1 at the penumbra compared with the MCAO group, indicating that autophagic initiation was enhanced by EE. We also revealed that EE therapy markedly increased the ratio of LC3-II/LC3-I. LC3-I reflects basal autophagy, while LC3-II represents autophagosome formation, and the ratio of LC3-II/LC3-I indicates the extent of autophagic activation (Kabeya et al., 2000). Thus, the increased LC3-II/LC3-I ratio in the MCAO + EE group in the present study suggests that autophagic activity was reinforced by EE treatment. However, the enhancement of autophagic activity inevitably results in the increased production of autophagic cargoes, which is an important cause of neuronal cytotoxicity after cerebral stroke (Cavaliere et al., 2019). We therefore evaluated the status of the subsequent steps in the autophagic flux pathway. Our results illustrated that the autophagic substrates of insoluble p62 and ubiquitin were significantly reduced in the MCAO + EE group compared with the MCAO group. Moreover, EE treatment also improved lysosomal function, reflected by the increased expressions of LAMP-1, cathepsin B, and cathepsin D. These results suggest that EE-induced increases in autophagic substrates can be effectively digested by the enhanced lysosomal capacity that occurs with this treatment. In addition, we simultaneously investigated the efficacy of EE

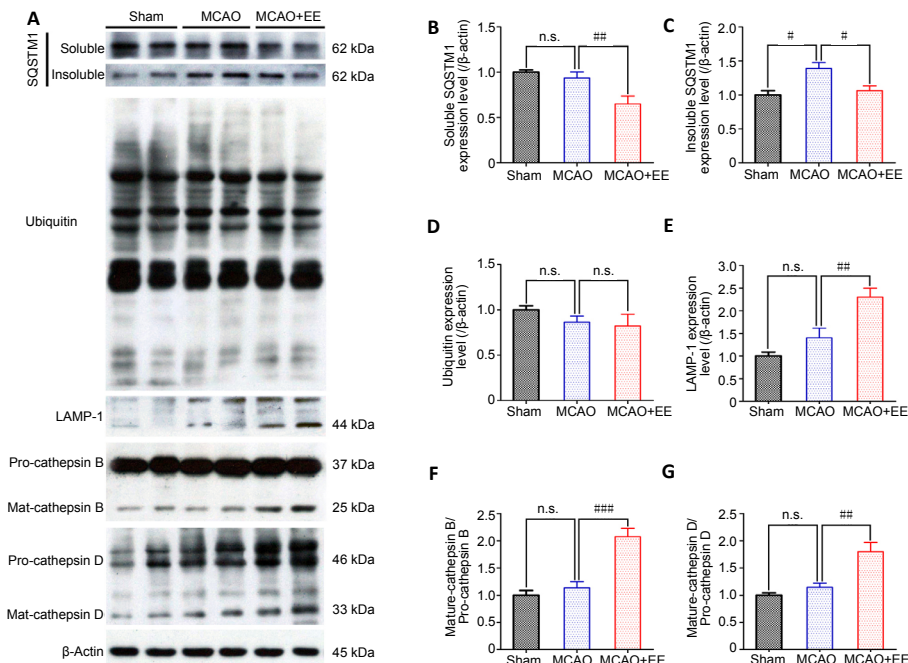
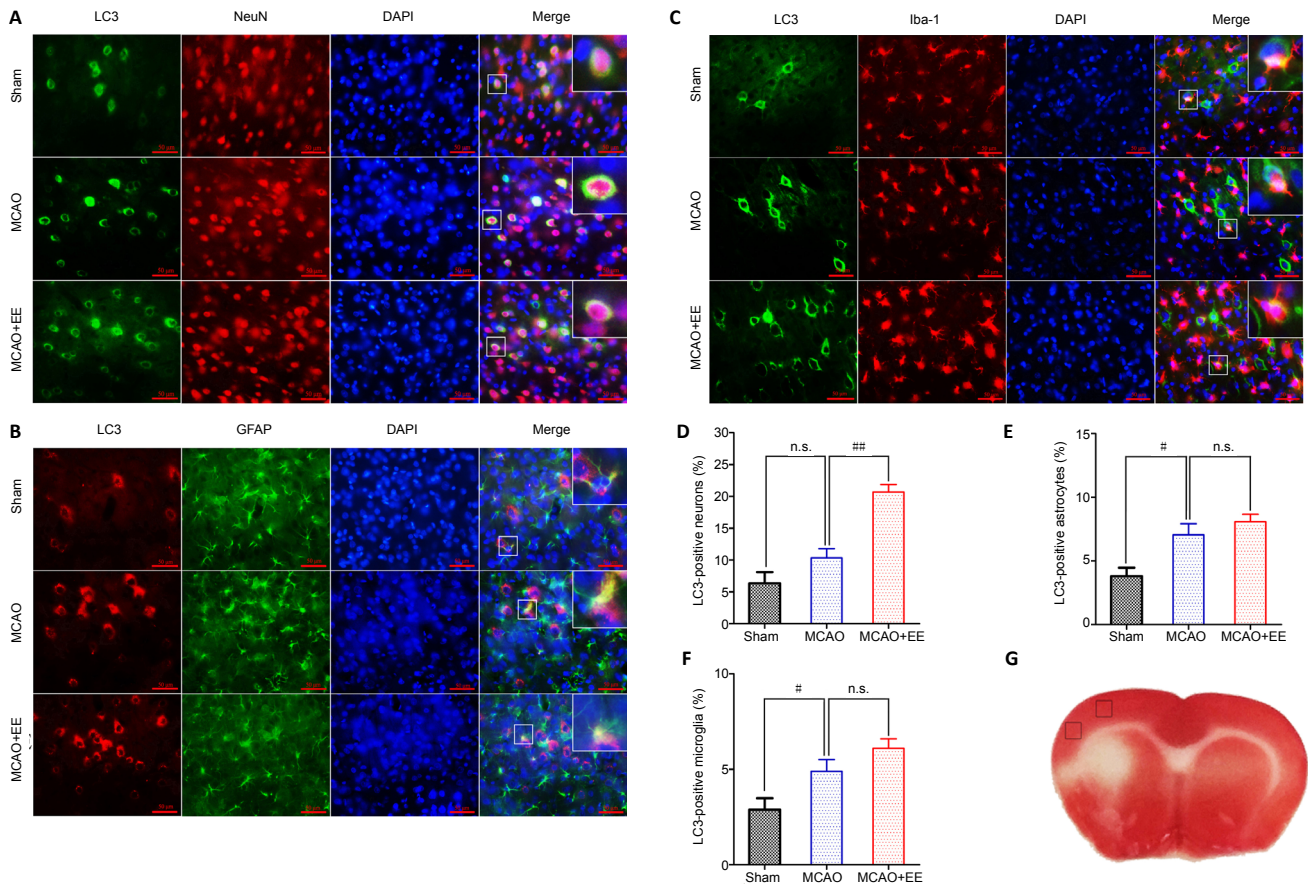


Figure 4 | Proteins in the autophagic/lysosomal pathway are detected in the penumbra of ischemic stroke rats to evaluate the efficacy of EE treatment on autophagic flux.

MCAO + EE group: MCAO animals were housed in EE cages; MCAO group: MCAO rats were housed in standard cages; sham group: the sham surgery rats were housed in EE cages. (A) Protein bands. (B–G) Quantitative results of proteins in the autophagic/lysosomal pathway. Data are expressed as the mean \pm SEM of the ratio to the sham group ($n = 6$). $\#P < 0.05$, $\#\#\#P < 0.001$ (one-way analysis of variance followed by Dunnett’s test). EE: Enriched environment; LAMP-1: lysosomal-associated membrane protein 1; LC3: light chain 3; MCAO: middle cerebral artery occlusion; n.s.: no significance; SQSTM1: sequestosome 1.

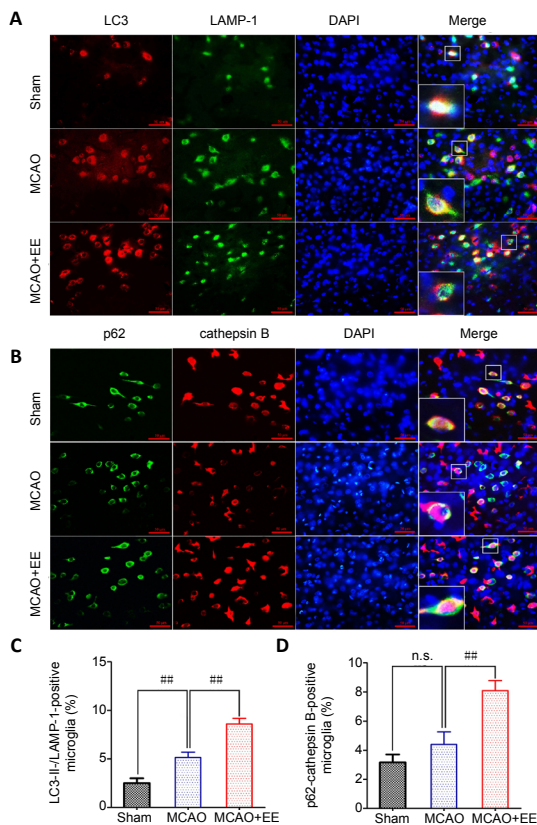


Figure 5 | Effects of EE treatments on autolysosomal function in the penumbra of ischemic stroke rats as evaluated by double immunofluorescence.

MCAO + EE group: MCAO animals were housed in EE cages; MCAO group: MCAO rats were housed in standard cages; sham group: the sham surgery rats were housed in EE cages. (A, B) The ratios of LC3-II-/LAMP-1- and p62-/cathepsin B-positive cells were markedly increased in the MCAO + EE group compared with the MCAO group. This implied that EE treatment was not only able to boost the fusion of autophagosomes with lysosomes, but could also enhance autophagic degradation. Green (stained by Alexa Fluor-488) indicates LAMP-1 and p62; red (stained by Alexa Fluor-594) indicates LC3 and cathepsin B; blue indicates total cells; and yellow indicates LC3-II-/LAMP-1- and p62-/cathepsin B-positive cells. Scale bars: 50 μ m. (C, D) Quantitative results of LC3-II-LAMP-1- and p62-cathepsin B-positive cells. Data are expressed as the mean \pm SEM of the ratio to the sham group ($n = 6$). $###P < 0.01$ (one-way analysis of variance followed by Dunnett's test). DAPI: 4',6-Diamidino-2-phenylindole; EE: enriched environment; LAMP1: lysosomal-associated membrane protein 1; LC3: light chain 3; MCAO: middle cerebral artery occlusion; n.s.: no significance.

treatment on autophagic flux using immunofluorescence. Our results demonstrated that EE-induced increases in autophagic activity mainly occurred in neurons. The percentages of LC3-II-/LAMP-1- and p62-/cathepsin B-positive cells in the MCAO + EE group were significantly higher than those in the MCAO group, indicating that EE treatment facilitates the fusion of autophagosomes with lysosomes. Thus, our study showed that EE not only increased autophagic activity, but also enhanced autophagic degradation.

In conclusion, the present research investigated whether the neuroprotective efficacy of EE treatment to facilitate rehabilitation from ischemic stroke was elicited by modulating the autophagic/lysosomal pathway. The results demonstrated that EE treatment was not only able to reinforce autophagic activity, reflected by elevated Beclin-1 and LC3-II expressions, but was also able to ameliorate cerebral ischemia-induced lysosomal dysfunction, reflected by enhanced lysosomal activity and reduced accumulation of autophagic substrates. We therefore concluded that EE treatment boosts recovery from ischemic stroke by facilitating autophagic flux.

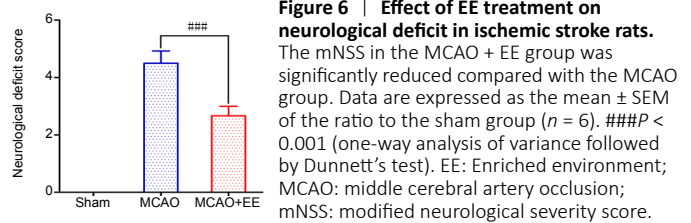


Figure 6 | Effect of EE treatment on neurological deficit in ischemic stroke rats. The mNSS in the MCAO + EE group was significantly reduced compared with the MCAO group. Data are expressed as the mean \pm SEM of the ratio to the sham group ($n = 6$). $###P < 0.001$ (one-way analysis of variance followed by Dunnett's test). EE: Enriched environment; MCAO: middle cerebral artery occlusion; mNSS: modified neurological severity score.

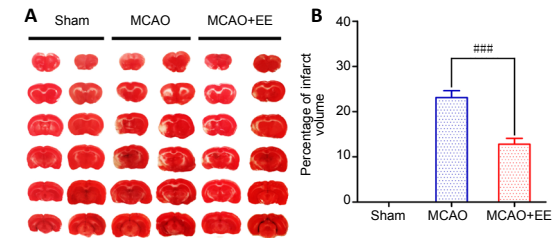


Figure 7 | Effects of EE treatment on infarct volume in ischemic stroke rats.

MCAO + EE group: MCAO animals were housed in EE cages; MCAO group: MCAO rats were housed in standard cages; sham group: the sham surgery rats were housed in EE cages. (A) With TTC staining, normal brain tissue is red and infarct tissue is pale. Infarct volume was attenuated by 4 weeks of EE treatment compared with the MCAO group. (B) Quantitative results of the percentage of infarct volume. Data are expressed as the mean \pm SEM of the ratio to the sham group ($n = 6$). $###P < 0.001$ (one-way analysis of variance followed by Dunnett's test). EE: Enriched environment; MCAO: middle cerebral artery occlusion; TTC: triphenyltetrazolium chloride.

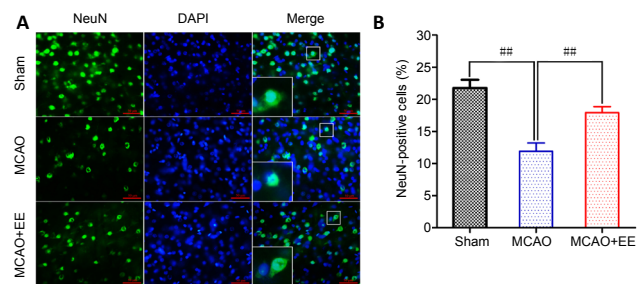


Figure 8 | Effects of EE treatment on neuronal survival in the penumbra of ischemic stroke rats as assessed by immunofluorescence.

MCAO + EE group: MCAO animals were housed in EE cages; MCAO group: MCAO rats were housed in standard cages; sham group: the sham surgery rats were housed in EE cages. (A) The percentage of NeuN-positive cells in the MCAO + EE group was significantly higher than in the MCAO group. Green (stained by Alexa Fluor-488) indicates NeuN-positive cells; blue indicates total cells. Scale bars: 50 μ m. (B) Quantitative results of the percentage of NeuN-positive cells. Data are expressed as the mean \pm SEM of the ratio to the sham group ($n = 6$). $###P < 0.01$ (one-way analysis of variance followed by Dunnett's test). DAPI: 4',6-Diamidino-2-phenylindole; EE: enriched environment; MCAO: middle cerebral artery occlusion.

Our study preliminarily explored the neuroprotective efficacy of EE to alleviate cerebral ischemia/reperfusion injury. Our results provide new insights into rehabilitation treatments after ischemic stroke. Moreover, our findings can be applied to the clinic, because clinical patients can also be treated with an integrated environment, similar to EE, to boost recovery from stroke. This combined environment may include early exercise, close social contact, an interesting natural environment, appropriately challenging tasks, and certain physical activities. However, the present study only explored the effects of EE treatment on whole autophagic flux; thus, further studies are needed to elucidate its underlying mechanisms. Furthermore, in this experiment, there may be errors caused by individual differences in the rats. This error can be reduced by enlarging the number of animals used in each experiment. In future research, we will also investigate the specific efficacy of EE in each step of the autophagic/lysosomal pathway, using regulators of autophagic flux signaling. Thus, novel therapeutic clues targeting autophagic flux may be found to facilitate post-stroke rehabilitation.

Author contributions: *Study design and concept: YHD, HYH; literature search and experimental implementation: YHD, LLD, HYH; data acquisition: LLD, YJZ, XMZ; statistical analysis: YHD, LLD, YJZ, XMZ, HYH; manuscript writing: YHD, HYH. All authors approved the final version of the manuscript.*

Conflicts of interest: *The authors declare that they have no conflict of interests.*

Financial support: *This work was supported by the National Natural Science Foundation of China, Nos. 81660383 (to YHD), 81860411 (to HYH), 81960418 (to YHD); Yunnan Ten Thousand Talents Plan Young & Elite Talents Project of China, No. YNWR-QNBJ-2018-034 (to YHD); Applied Basic Research Foundation of Yunnan Province of China, Nos. 2017FB113 (to YHD), 2019FB098 (to HYH); and Science Research Fund of Yunnan Provincial Department of Education of China, No. 2018JS016 (to HYH). The funders had no roles in the study design, conduction of experiment, data collection and analysis, decision to publish, or preparation of the manuscript.*

Institutional review board statement: *The study was approved by the Animal Experiment Committee of Kunming University of Science and Technology (approval No. 5301002013855) on March 1, 2019.*

Copyright license agreement: *The Copyright License Agreement has been signed by all authors before publication.*

Data sharing statement: *Datasets analyzed during the current study are available from the corresponding author on reasonable request.*

Plagiarism check: *Checked twice by iThenticate.*

Peer review: *Externally peer reviewed.*

Open access statement: *This is an open access journal, and articles are distributed under the terms of the Creative Commons Attribution-NonCommercial-ShareAlike 4.0 License, which allows others to remix, tweak, and build upon the work non-commercially, as long as appropriate credit is given and the new creations are licensed under the identical terms.*

References

Benjamin EJ, Muntner P, Alonso A, Bittencourt MS, Callaway CW, Carson AP, Chamberlain AM, Chang AR, Cheng S, Das SR, Delling FN, Djousse L, Elkind MSV, Ferguson JF, Fornage M, Jordan LC, Khan SS, Kissela BM, Knutson KL, Kwan TW, et al. (2019) Heart Disease and Stroke Statistics-2019 update: A report from the American Heart Association. *Circulation* 139:e56-e528.

Button RW, Luo S, Rubinshtein DC (2015) Autophagic activity in neuronal cell death. *Neurosci Bull* 31:382-394.

Cavaliere F, Fornarelli A, Bertan F, Russo R, Marsal-Cots A, Morrone LA, Adornetto A, Corasaniti MT, Bano D, Bagetta G, Nicotera P (2019) The tricyclic antidepressant clomipramine inhibits neuronal autophagic flux. *Sci Rep* 9:4881.

Chen X, Zhang X, Liao W, Wan Q (2017a) Effect of physical and social components of enriched environment on astrocytes proliferation in rats after cerebral ischemia/reperfusion injury. *Neurochem Res* 42:1308-1316.

Chen X, Zhang X, Xue L, Hao C, Liao W, Wan Q (2017b) Treatment with enriched environment reduces neuronal apoptosis in the periinfarct cortex after cerebral ischemia/reperfusion injury. *Cell Physiol Biochem* 41:1445-1456.

Connell LA, Smith MC, Byblow WD, Stinear CM (2018) Implementing biomarkers to predict motor recovery after stroke. *NeuroRehabilitation* 43:41-50.

Farrell R, Evans S, Corbett D (2001) Environmental enrichment enhances recovery of function but exacerbates ischemic cell death. *Neuroscience* 107:585-592.

Galluzzi L, Bravo-San Pedro JM, Blomgren K, Kroemer G (2016) Autophagy in acute brain injury. *Nat Rev Neurosci* 17:467-484.

Gao BY, Sun CC, Xia GH, Zhou ST, Zhang Y, Mao YR, Liu PL, Zheng Y, Zhao D, Li XT, Xu J, Xu DS, Bai YL (2020) Paired associated magnetic stimulation promotes neural repair in the rat middle cerebral artery occlusion model of stroke. *Neural Regen Res* 15:2047-2056.

Gatica D, Lahiri V, Klionsky DJ (2018) Cargo recognition and degradation by selective autophagy. *Nat Cell Biol* 20:233-242.

Gonçalves LV, Herlinger AL, Ferreira TAA, Coitinho JB, Pires RGW, Martins-Silva C (2018) Environmental enrichment cognitive neuroprotection in an experimental model of cerebral ischemia: biochemical and molecular aspects. *Behav Brain Res* 348:171-183.

Hakon J, Quattromani MJ, Sjölund C, Tomasevic G, Carey L, Lee JM, Ruscher K, Wieloch T, Bauer AQ (2018) Multisensory stimulation improves functional recovery and resting-state functional connectivity in the mouse brain after stroke. *Neuroimage Clin* 17:717-730.

Han D, Kwon M, Lee SM, Pleasure SJ, Yoon K (2020) Non-cell autonomous promotion of astrogenesis at late embryonic stages by constitutive YAP activation. *Sci Rep* 10:7041.

He HY, Ren L, Guo T, Deng YH (2019) Neuronal autophagy aggravates microglial inflammatory injury by downregulating CX3CL1/fractalkine after ischemic stroke. *Neural Regen Res* 14:280-288.

Jeffers MS, Corbett D (2018) Synergistic effects of enriched environment and task-specific reach training on poststroke recovery of motor function. *Stroke* 49:1496-1503.

Kabeya Y, Mizushima N, Ueno T, Yamamoto A, Kirisako T, Noda T, Kominami E, Ohsumi Y, Yoshimori T (2000) LC3, a mammalian homologue of yeast Apg8p, is localized in autophagosomal membranes after processing. *EMBO J* 19:5720-5728.

Kaminsky V, Zhivotovsky B (2012) Proteases in autophagy. *Biochim Biophys Acta* 1824:44-50.

Krueger H, Koot J, Hall RE, O'Callaghan C, Bayley M, Corbett D (2015) Prevalence of individuals experiencing the effects of stroke in Canada: Trends and projections. *Stroke* 46:2226-2231.

Lahiri V, Hawkins WD, Klionsky DJ (2019) Watch what you (Self-) eat: autophagic mechanisms that modulate metabolism. *Cell Metab* 29:803-826.

Langhorne P, Wu O, Rodgers H, Ashburn A, Bernhardt J (2017) A Very Early Rehabilitation Trial after stroke (AVERT): a phase III, multicentre, randomised controlled trial. *Health Technol Assess* 21:1-120.

Leng T, Xiong ZG (2019) Treatment for ischemic stroke: From thrombolysis to thrombectomy and remaining challenges. *Brain Circ* 5:8-11.

Malá H, Rasmussen CP (2017) The effect of combined therapies on recovery after acquired brain injury: Systematic review of preclinical studies combining enriched environment, exercise, or task-specific training with other therapies. *Restor Neurol Neurosci* 35:25-64.

Mering S, Jolkonen J (2015) Proper housing conditions in experimental stroke studies-special emphasis on environmental enrichment. *Front Neurosci* 9:106.

Mo J, Enkhjargal B, Travis ZD, Zhou K, Wu P, Zhang G, Zhu Q, Zhang T, Peng J, Xu W, Ocak U, Chen Y, Tang J, Zhang J, Zhang JH (2019) AVE 0991 attenuates oxidative stress and neuronal apoptosis via Mas/PKA/CREB/UCP-2 pathway after subarachnoid hemorrhage in rats. *Redox Biol* 20:75-86.

Montalván Ayala V, Rojas Cheje Z, Aldave Salazar R (2018) Controversies in cerebrovascular disease: High or low doses of recombinant tissue plasminogen activator to treat acute stroke? A literature review. *Neurologia* doi:10.1016/j.nrl.2018.04.003.

Pengyue Z, Tao G, Hongyun H, Liqiang Y, Yihao D (2017) Breviscapine confers a neuroprotective efficacy against transient focal cerebral ischemia by attenuating neuronal and astrocytic autophagy in the penumbra. *Biomed Pharmacother* 90:69-76.

Qian HZ, Zhang H, Yin LL, Zhang JJ (2018) Posts ischemic Housing Environment on Cerebral Metabolism and Neuron Apoptosis after Focal Cerebral Ischemia in Rats. *Curr Med Sci* 38:656-665.

Skowrońska K, Obara-Michlewska M, Czarnecka A, Dąbrowska K, Zielińska M, Albrecht J (2019) Persistent overexposure to N-methyl-D-aspartate (NMDA) calcium-dependently downregulates glutamine synthetase, aquaporin 4, and Kir4.1 channel in mouse cortical astrocytes. *Neurotox Res* 35:271-280.

Sun Y, Zhang T, Zhang Y, Li J, Jin L, Sun Y, Shi N, Liu K, Sun X (2018) Ischemic postconditioning alleviates cerebral ischemia-reperfusion injury through activating autophagy during early reperfusion in rats. *Neurochem Res* 43:1826-1840.

Wang P, Shao BZ, Deng Z, Chen S, Yue Z, Miao CY (2018) Autophagy in ischemic stroke. *Prog Neurobiol* 163-164:98-117.

Wang W, Jiang B, Sun H, Ru X, Sun D, Wang L, Wang L, Jiang Y, Li Y, Wang Y, Chen Z, Wu S, Zhang Y, Wang D, Wang Y, Feigin VL (2017) Prevalence, incidence, and mortality of stroke in China: Results from a nationwide population-based survey of 480687 adults. *Circulation* 135:759-771.

Wang YZ, Zhang HY, Liu F, Li L, Deng SM, He ZY (2019) Association between PPARG genetic polymorphisms and ischemic stroke risk in a northern Chinese Han population: a case-control study. *Neural Regen Res* 14:1986-1993.

Wei K, Wang P, Miao CY (2012) A double-edged sword with therapeutic potential: an updated role of autophagy in ischemic cerebral injury. *CNS Neurosci Ther* 18:879-886.

Wright H, Wright T, Pohlig RT, Kasner SE, Raser-Schramm J, Reisman D (2018) Protocol for promoting recovery optimization of walking activity in stroke (PROWALKS): a randomized controlled trial. *BMC Neurol* 18:39.

Wu JZ, Ardah M, Haikal C, Svanbergsson A, Diepenbroek M, Vaikath NN, Li W, Wang ZY, Outeiro TF, El-Agnaf OM, Li JY (2019) Dihydropyridin and Salvianolic acid B inhibit alpha-synuclein aggregation and enhance chaperone-mediated autophagy. *Translational neurodegeneration* 8:18.

Yu K, Wu Y, Hu Y, Zhang Q, Xie H, Liu G, Chen Y, Guo Z, Jia J (2013) Neuroprotective effects of prior exposure to enriched environment on cerebral ischemia/reperfusion injury in rats: the possible molecular mechanism. *Brain Res* 1538:93-103.

Zhang X, Chen XP, Lin JB, Xiong Y, Liao WJ, Wan Q (2017) Effect of enriched environment on angiogenesis and neurological functions in rats with focal cerebral ischemia. *Brain Res* 1655:176-185.

Zhang Y, Xu D, Qi H, Yuan Y, Liu H, Yao S, Yuan S, Zhang J (2018) Enriched environment promotes post-stroke neurogenesis through NF- κ B-mediated secretion of IL-17A from astrocytes. *Brain Res* 1687:20-31.

Zhi X, Feng W, Rong Y, Liu R (2018) Anatomy of autophagy: from the beginning to the end. *Cell Mol Life Sci* 75:815-831.

C-Editor: Zhao M; S-Editors: Yu J, Li CH; L-Editors: Gardner D, Yu J, Suy CP; T-Editor: Jia Y